THE ASTROPHYSICAL JOURNAL, Vol. 151, January 1968

ROCKET ULTRAVIOLET SPECTROPHOTOMETRY IN THE ORION REGION

ALBERT BOGGESS III AND YOJI KONDO*
Goddard Space Flight Center, National Aeronautics and Space Administration, Greenbelt, Maryland
Received November 6, 1967

Low-resolution ultraviolet spectra of several bright stars in the region of Orion have been photographed from an Aerobee rocket launched at White Sands Missile Range on November 29, 1965. The intent was to obtain objectively dispersed spectrograms suitable for relative spectrophotometry of early-type stars. The rocket was fitted with an inertial guidance system capable of stabilizing the rocket to within about $\pm\frac{1}{4}°$, and, in order to improve the spectral resolution, the inertial error signal in the direction of dispersion was also used to drive a single-axis gimbal that supported the cameras. The resulting stability in that axis was approximately $\pm 3'$. Three cameras were flown. They were small Schmidt systems operating at T/1.0 with 28-mm focal lengths and 30° fields of view. The objective reflection gratings had 2160 lines/mm, producing a dispersion of 100 Å/mm near the field center. The cameras are capable of 5 Å resolution, but the jitter of the rocket platform limited their performance to about 10 Å. The camera systems are very similar to those described in detail by Morton and Spitzer (1966).

Exposures were made on two types of photographic film: the phosphor-coated IO-UV, and Schumann emulsion SC-V. The exposures on the SC-V film were superior due to its higher speed and finer grain, and most of the reduced data has been derived from these images. A variety of exposure times was used; the ones of 40-sec duration were optimum in terms of image density and background fog level. The rocket pointing control had been programmed to center the cameras on the Belt of Orion in order that the cameras could photograph the entire constellation. However, a malfunction in the slewing operation caused the rocket to point several degrees too far south, so that the northern part of the constellation was not recorded. On the other hand, spectra were obtained of stars in Canis Major that would not otherwise have been seen. A typical exposure is shown in Figure 1 (Plate L1).

The determination of wavelengths for objective grating spectra is a straightforward process. The zeroth-order images of faint stars can be used for direct measurements of plate scale. Wherever such an image is superimposed on the spectrum on another star, the wavelength of that point in the spectrum may be computed by calculating the angle between the two stars and multiplying it by the known angular dispersion of the grating. The wavelength scales produced in this way are found to have accuracies comparable to the spectral resolution. The usual problems arising from overlapping spectra are aggravated in these exposures due to the large angular dispersion of the grating and also because the spectral sensitivity of the silver halide grains extends so far into the visible, adding nearly 2000 Å of extraneous spectrum to each star. Results are quoted here only in those cases where a stellar spectrum is free from contamination across its whole width, permitting a measurement of the total energy received at that wavelength, or where the contamination would contribute less than 10 per cent to the measurement.

Changes in image aberrations across the field of view resulted in systematic changes in the widening of the spectra at different locations in the field. As a result, it was not possible to determine relative spectral distributions from a single densitometer trace of a spectrum. Instead, multiple traces were made using an automatically scanning micro-

* NASA National Academy of Sciences–National Research Council Postdoctoral Research Associate.

PLATE L1

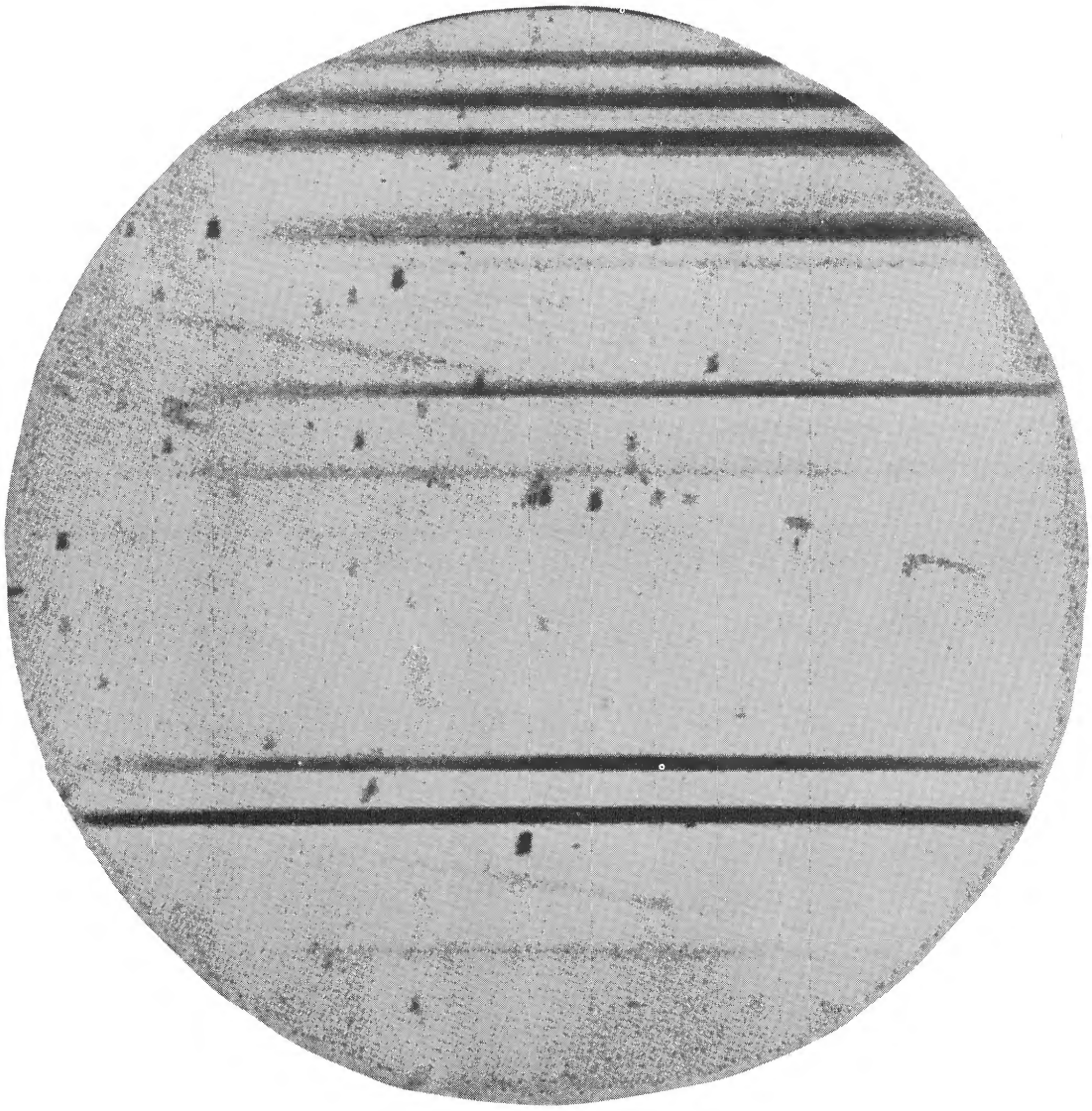

FIG. 1.—Ultraviolet spectrogram. The seven brightest spectra, from top to bottom, are δ Ori, ϵ Ori, ζ Ori, β Ori, κ Ori, β CMa, and α CMa. The short-wavelength limit on this exposure is about 1600 Å. The superimposed zeroth-order images of field stars are used to establish wavelength and evaluate guidance quality.

BOGGESS AND KONDO (*see* page L5)

densitometer with a digitized output. These traces produced a two-dimensional map of each spectrum which could then be integrated perpendicular to the direction of dispersion to find the total intensity at each wavelength. Conversion from photographic densities to intensities was accomplished via monochromatic calibrations at 2537 Å impressed on the flight film before and after flight. Characteristic curves for these types of film appear to be nearly wavelength independent (Fowler, Rense, and Simmons 1965). Finally, corrections were necessary to allow for changes in dispersion across the large field of view and to allow for vignetting due to the restricted size of the grating. The maximum vignetting correction was about 20 per cent at the long-wavelength end of a few spectra.

Table 1 gives results for those stars for which the data is most reliable. The wave-

TABLE 1

RELATIVE APPARENT MAGNITUDES WITH RESPECT TO α CANIS MAJORIS

Star	Sp.	V (mag)	Δm 1750 Å (mag)	Δm 2250 Å (mag)	Δm 2750 Å (mag)	Δm 1750−V (mag)	Δm 2250−V (mag)	Δm 2750−V (mag)
α CMa.....	A1 V	−1.47	0.0	0.0	0.0	−0.1	0.0	+0.2
β Ori.....	B8 Ia	0.08	.....	0.6	0.9	.....	−1.0	−0.5
ζ CMa.....	B2.5 V	3.02	1.3	.....	.....	−3.3	.....	.....
γ Ori.....	B2 III	1.64	.....	0.7	.....	.....	−2.4	.....
β CMa.....	B1 II	1.98	0.6	0.6	.....	−3.0	−2.9	.....
κ Ori.....	B0.5 Ie	2.04	0.7	0.8	1.3	−2.9	−2.7	−2.0
ξ CMa.....	B0.5 IV	4.33	.....	.....	3.3	.....	.....	−2.3
η Ori.....	B0.5 V	3.35	.....	2.0	2.7	.....	−2.8	−1.9
ε Ori.....	B0 Ia	1.70	0.1	0.3	0.9	−3.2	−2.9	−2.1
ν Ori.....	B0 V	4.63	2.6	2.9	.....	−3.6	−3.2	.....
ζ Ori.....	O9.5 Ib	2.05	0.2	0.5	1.1	−3.4	−3.0	−2.2
δ Ori.....	O9.5 II	2.20	0.7	0.8	1.4	−3.1	−2.9	−2.1

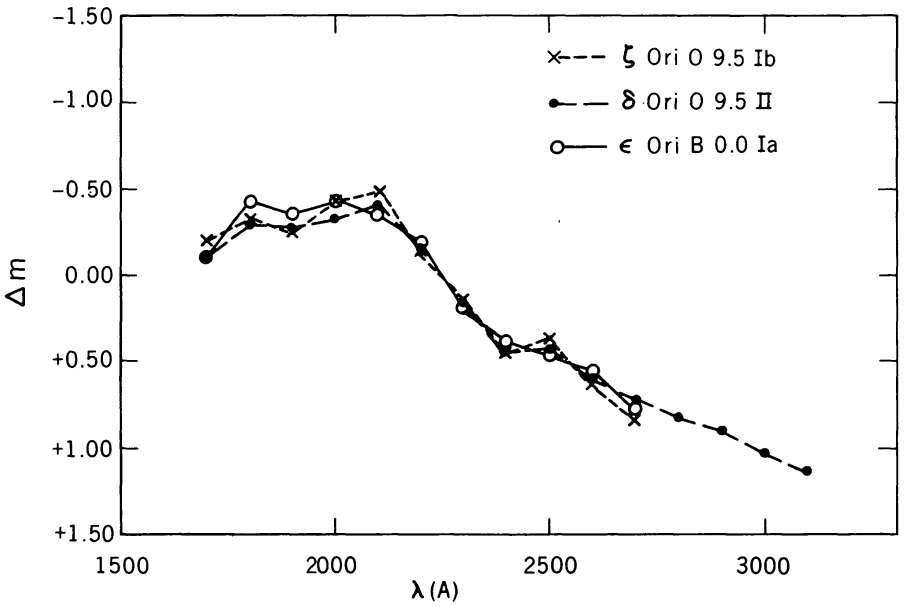

FIG. 2.—Ultraviolet spectral energy distributions. Plotted points represent 100 Å averages and have been normalized at 2250 Å.

lengths 1750, 2250, and 2750 Å have been chosen as representative, and the stellar brightnesses averaged over 100 Å intervals are given relative to the brightness of α CMa. The data are estimated to be good to one-tenth magnitude. Although several of these stars have suspected variability, it is smaller than the uncertainty quoted here in every case. The stars η Ori and δ Ori are eclipsing binaries. Both were out of eclipse at the time of observation. The star δ Ori has a B2 companion which may be neglected since its visual magnitude is 4.7 magnitudes fainter than the O9.5 primary. Similarly, the B3 companion of ζ Ori is 2.2 mag fainter than the O9.5 primary and may be disregarded. By making use of Stecher's absolute spectrophotometry of α CMa, the relative data may be converted to true energy distribution. These energy distributions are tabulated in the last three columns of Table 1. More detailed spectra are shown in Figures 2 and 3 for

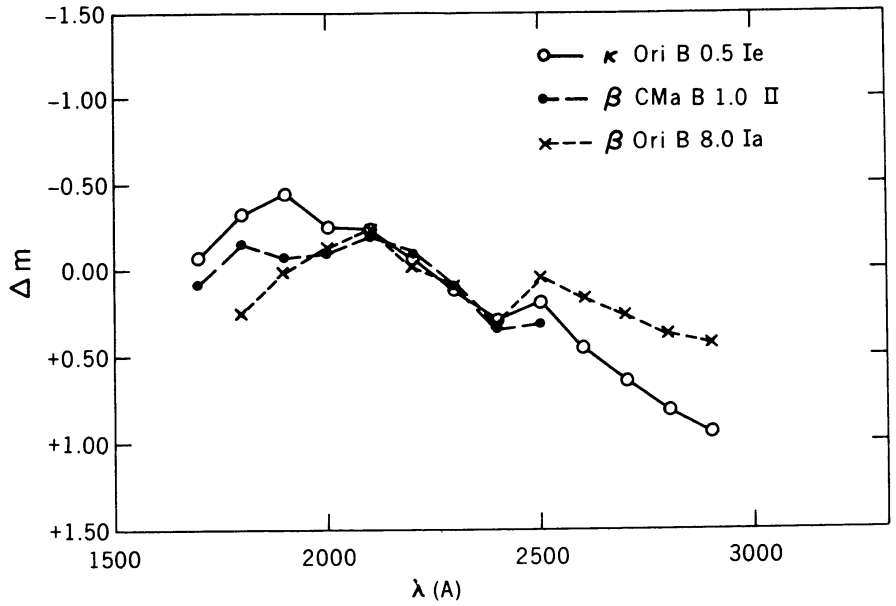

FIG. 3.—Ultraviolet spectral energy distributions. Plotted points represent 100 Å averages and have been normalized at 2250 Å.

six of the stars that were best observed. In these figures, the magnitude differences have been normalized to zero at 2250° Å. Figure 2 shows the spectral distributions for three supergiants of spectral types O9.5 and B0, and it may be seen that they agree to within observational error. In Figure 3 somewhat later B supergiants are shown, and their energy distributions are, at least qualitatively, as may be expected from their temperatures, i.e., more energy is radiated in the shorter wavelengths in stars of earlier spectral types.

No corrections for interstellar extinction have been made to these data.

REFERENCES

Fowler, W. K., Rense, W. A., and Simmons, W. R. 1965, *Appl. Opt.*, **4**, 1596.
Morton, D. C., and Spitzer, L., Jr. 1966, *Ap. J.*, **144**, 1.